Theory of Polydisperse Inhomogeneous Polymers

Glenn H. Fredrickson*,† and Scott W. Sides‡

Departments of Chemical Engineering & Materials and Department of Chemical Engineering, University of California, Santa Barbara, California 93106-5080

Received January 22, 2003; Revised Manuscript Received May 12, 2003

ABSTRACT: A formalism is presented for incorporating realistic molecular weight distributions into field theory models of inhomogeneous polymeric fluids. The method is illustrated in the context of an equilibrium interface between coexisting phases of molten polydisperse A and B homopolymers. We solve the model field theory in the self-consistent mean-field approximation and analyze the structure of the interface for the special case of a Schulz molecular weight distribution. The formalism is general, however, and can be used even beyond the mean-field approximation to assess polydispersity effects in a wide variety of inhomogeneous polymers, such as block and graft copolymers and their alloys.

1. Introduction

Field-theoretic models and approaches have proven to be extremely useful in the study of inhomogeneous polymer and complex fluid phases. The application of such methods to dense phases, such as melts and concentrated solutions of homo, block, and graft copolymers, has been particularly fruitful in unravelling the complexities of equilibrium self-assembly in such systems.[1−5] Normally the statistical field theory models are solved in the mean-field (saddle point) approximation, although recent developments enable direct numerical simulation of field theories without any simplifying approximations.[6,7]

Commercial polymer alloys, block copolymers, and graft copolymers are characterized by various types of "chemical disorder" that reflect the statistical nature of the polymerization, branching, and coupling processes that are used to manufacture the materials.[8] This disorder can take several forms, including simple polydispersity, in which component polymers, blocks or grafts, possess a distribution of molecular weights. Other types of chemical disorder include sequence distributions in statistical copolymers and "architectural disorder" in which macromolecules have a distribution of topologies by virtue of statistical branching, grafting, or coupling processes. Even materials that are prepared under carefully controlled reaction conditions, e.g., anionic polymerization, and are intended for model laboratory studies contain substantial amounts of disorder that can sometimes have surprising consequences.[9] Moreover, chemical disorder can be intentionally introduced to create novel self-assembled structures of practical value.[10]

Previous attempts have been made to incorporate chemical disorder into statistical field theory models of inhomogeneous polymeric fluids. Models have been introduced to describe statistical AB copolymers, statistical AB multiblock copolymers, and statistical AB graft copolymers, including sequence correlations.[11−17] However, these models have generally not included polydispersity intrinsic to the overall chains, grafts, or blocks and have been solved only approximately—generally within the weak segregation, mean-field approximation. Realistic polydispersity has been approximately incorporated only in the context of weak segregation expansions for simple AB block copolymers and binary blends[18−20] and in the strong segregation limit of mean-field theory.[21] Very recently, Pagonabarraga and Cates[22] proposed an approximate density functional for polydisperse polymers, connecting to effective particle concepts and weak segregation and weak gradient expansions. The few studies that have avoided such analytical approximations, instead employing numerical self-consistent mean-field theory (SCMFT), have utilized simple bimodal (sum of two delta functions) distributions of molecular weight.[23,24] It would clearly be highly desirable to have a scheme for embedding continuous distributions of chain lengths into equilibrium calculations for inhomogeneous polymers that is in principle exact and not dependent on simplifying approximations, such as weak or strong segregation expansions and even the mean-field approximation. For a recent review of the treatment of polydispersity effects in the equilibrium phase behavior of *homogeneous* polymeric fluids, we refer the interested reader to an article by Sollich.[25]

In the present paper, we show how realistic continuous chain length distributions can be incorporated into statistical field theory models of inhomogeneous polymers. These models can be solved either in the mean-field approximation (SCMFT) or by numerical simulation of the exact field theory, i.e., a "field-theoretic polymer simulation" (FTPS).[7] To illustrate the approach, we use numerical SCMFT to examine the equilibrium structure of the melt interface between coexisting phases of polydisperse A and B homopolymers. We show how to compute the equilibrium structure of the interface, including the density profile of any component in the chain length distribution. As a simple test case, we treat a symmetric interface where the molecular weight distributions of the A and B chains are identical and employ a Schulz expression for the distribution function. The formalism can be extended in a straightforward manner to other types of polydisperse systems, including more complex alloys containing block and graft copolymers.

† Departments of Chemical Engineering & Materials.
‡ Department of Chemical Engineering.
* Corresponding author. E-mail ghf@mrl.ucsb.edu.

10.1021/ma034082y CCC: $25.00
Published on Web 06/14/2003

II. Polydisperse Blend Model

In the present paper we consider a melt blend of type A and type B linear, flexible homopolymers in which both species have prescribed distributions of chain length. In developing the model, we closely follow the approach and notation of a recent review on field-theoretic simulation methods.[7] Polymers are described by continuous space curves, and we employ a canonical ensemble in which n_A type A chains and n_B type B chains are confined to a volume V. Conformations of noninteracting polymers are given a Gaussian statistical weight, $\exp(-U_0)$, where U_0 is the "Edwards Hamiltonian" (expressed in units of k_BT):[26]

$$U_0[\mathbf{R}_A,\mathbf{R}_B] = \frac{3}{2b_A^2}\sum_{\alpha=1}^{n_A}\int_0^{N_{\alpha A}} ds\, \left|\frac{d\mathbf{R}_{\alpha A}(s)}{ds}\right|^2 + \frac{3}{2b_B^2}\sum_{\alpha=1}^{n_B}\int_0^{N_{\alpha B}} ds\, \left|\frac{d\mathbf{R}_{\alpha B}(s)}{ds}\right|^2 \quad (1)$$

In this expression $\mathbf{R}_{\alpha K}(s)$ denotes a space curve describing the conformation of the αth chain of type K (K = A or B), b_K is the statistical segment length of chains of species K, and $N_{\alpha K}$ is the degree of polymerization of the αth chain of type K. The nonbonded interactions among monomers in the model can be expressed in terms of microscopic monomer densities defined by $\hat{\rho}_K(\mathbf{r}) = \sum_{\alpha=1}^{n_K}\int_0^{N\alpha_K} ds\, \delta(\mathbf{r} - \mathbf{R}_{\alpha K}(s))$. There are two types of nonbonded interactions that are important to capture. The first is the tendency for a preference of similar (A−A and B−B) binary monomer contacts over dissimilar (A−B) contacts in the blend. This tendency can be described by a simple quadratic form

$$U_1[\mathbf{R}_A,\mathbf{R}_B] = v_0\chi\int d\mathbf{r}\, \hat{\rho}_A\hat{\rho}_B \quad (2)$$

familiar in Flory−Huggins theory, where χ is the Flory parameter.[27] We have conveniently defined monomers (statistical segments) so that they occupy the same volume in the melt,[28] i.e., $v_A = v_B \equiv v_0$. The total average monomer density is given by $\rho_0 \equiv 1/v_0$.

The second type of nonbonded interactions that are important to include in a model of polymer melts are the harshly repulsive interactions that lead to small variations in total monomer density on meso- and macroscales. A simple way to incorporate such interactions is through a strict "incompressible melt" approximation,[3,27] which is imposed by a functional delta $\delta(\hat{\rho}_A + \hat{\rho}_B - \rho_0)$ that forces the sum of the two microscopic monomer densities, $\hat{\rho}_A(\mathbf{r}) + \hat{\rho}_B(\mathbf{r})$, to be equal to the average total density ρ_0 at each point $\mathbf{r}$ in the system. Assembling all three types of interactions produces the following "microscopic" model of a molten binary polymer blend:

$$Z = \int\mathscr{D}[\mathbf{R}_A]\int\mathscr{D}[\mathbf{R}_B]\, \delta(\hat{\rho}_A + \hat{\rho}_B - \rho_0)\exp(-U_0 - U_1) \quad (3)$$

where Z is the configurational partition function and the notation $\int\mathscr{D}[\mathbf{R}_K]$ denotes a set of path integrals over all possible conformations of the chains of species K.

The next task is to convert this model involving $n_A + n_B$ chain conformation path integrals into a field theory where the fundamental degrees of freedom are fluctuating chemical potential fields. This can be accomplished by giving the functional delta constraint an exponential representation and by introducing a Hubbard−Stratonovich transformation to decouple the pair interactions manifest in U_1. We omit the details and refer the reader to the literature.[1,3,7,29,30] The result can be written

$$Z = \int\mathscr{D}[w_A]\int\mathscr{D}[w_B]\exp(-H[w_A,w_B]) \quad (4)$$

with an effective Hamiltonian given by

$$H[w_A,w_B] = \rho_0\int d\mathbf{r}\,[-fw_A - (1-f)w_B + 1/(4\chi)(w_B - w_A)^2] - \sum_{\alpha=1}^{n_A}\ln Q_A(N_{\alpha A};[w_A]) - \sum_{\alpha=1}^{n_B}\ln Q_B(N_{\alpha B};[w_B]) \quad (5)$$

In the above expression, f denotes the average volume fraction of type A monomers in the system and $w_K(\mathbf{r})$ (K = A or B) is a fluctuating chemical potential field conjugate to the local density of monomers of species K at position $\mathbf{r}$. The paths of (functional) integration over the w_K fields in eq 4 are complex: $w_A - w_B$ is integrated along the real axis, and $w_A + w_B$ is integrated along the purely imaginary axis.

The functional $Q_K(N;[w_K])$ represents the partition function of a single type K polymer of length N in a chemical potential field $w_K(\mathbf{r})$. This object can be expressed in the form of a single chain path integral

$$Q_K(N;[w_K]) = \frac{\int\mathscr{D}[\mathbf{R}]\exp[-U_0 - \int_0^N ds\, w_K(\mathbf{R}(s))]}{\int\mathscr{D}[\mathbf{R}]\exp[-U_0]} \quad (6)$$

The path integral can be evaluated deterministically by the formula $Q_K(N;[w_K]) = V^{-1}\int d\mathbf{r}\, q_K(\mathbf{r},N)$, where $q_K(\mathbf{r},s)$ satisfies

$$\frac{\partial}{\partial s}q_K(\mathbf{r},s) = \frac{b_K^2}{6}\nabla^2 q_K(\mathbf{r},s) - w_K(\mathbf{r})\, q_K(\mathbf{r},s) \quad (7)$$

subject to the initial condition $q_K(\mathbf{r},0) = 1$. Clearly q_K is a functional of the field $w_K(\mathbf{r})$, although we suppress this in our notation.

In the thermodynamic limit ($n_K \to \infty$, $V \to \infty$, n_K/V finite), and assuming that the chains are long enough on average that the discrete distributions of chain lengths can be replaced by continuous distributions, the sums over polymer chains in eq 5 can be replaced by integrals over the chain length distribution functions of the two species:

$$H[w_A,w_B] = \rho_0\int d\mathbf{r}\,[-fw_A - (1-f)w_B + 1/(4\chi)(w_B - w_A)^2] - n_A\int_0^\infty dN\, p_A(N)\ln Q_A(N;[w_A]) - n_B\int_0^\infty dN\, p_B(N)\ln Q_B(N;[w_B]) \quad (8)$$

The quantity $n_K p_K(N)\, dN$ describes the number of type K chains in the system that have lengths between N and $N + dN$. The chain length distribution functions $p_K(N)$ are evidently normalized such that $\int_0^\infty dN\, p_K(N) = 1$. Also important are the first moments of the

distributions, reflecting the (number) average chain lengths

$$\bar{N}_K \equiv \int_0^\infty \mathrm{d}N\ N p_K(N) \tag{9}$$

With this notation, the average density of type K monomers can be expressed as $\rho_{K0} = n_K \bar{N}_K / V$, the total average monomer density is $\rho_0 = \rho_{A0} + \rho_{B0} = 1/v_0$, and the average volume fraction of species A is $f = \rho_{A0}/\rho_0$.

Equations 4 and 8 constitute the relevant field theory model for an incompressible blend of A and B homopolymers with arbitrary chain length distributions $p_K(N)$. To calculate with the model, we must express desired observables as functionals of the fluctuating w_K fields. Of particular interest are local density operators for monomers of each species. The *total* density of monomers of type K can be obtained by taking a first functional derivative with respect to the conjugate chemical potential field w_K

$$\rho_K(\mathbf{r}; [w_K]) = -n_K \int_0^\infty \mathrm{d}N\ p_K(N) \frac{\delta \ln Q_K(N; [w_K])}{\delta w_K(\mathbf{r})} \tag{10}$$

Invoking a well-known factorization of the path integral expression for Q_K,[31] the right-hand side can be rewritten in terms of q_K

$$\rho_K(\mathbf{r}; [w_K]) = \frac{n_K}{V} \int_0^\infty \mathrm{d}N\ \frac{p_K(N)}{Q_K(N; [w_K])} \int_0^N \mathrm{d}s\ q_K(\mathbf{r}, s)\ q_K(\mathbf{r}, N - s) \tag{11}$$

The local density of *monomers contributed by type K chains of length N* is given by a similar formula

$$\rho_K(N, \mathbf{r}; [w_K]) = \frac{n_K p_K(N)}{V Q_K(N; [w_K])} \int_0^N \mathrm{d}s\ q_K(\mathbf{r}, s)\ q_K(\mathbf{r}, N - s) \tag{12}$$

where evidently $\rho_K(\mathbf{r}) = \int_0^\infty \mathrm{d}N\ \rho_K(N, \mathbf{r})$. Equations 10−12 are density *operators* in the sense that an expectation value with respect to the fluctuating chemical potential fields yields the observable average density, e.g.

$$\langle \rho_K(\mathbf{r}; [w_K]) \rangle \equiv Z^{-1} \int \mathscr{D}[w_A] \int \mathscr{D}[w_B]\ \exp(-H[w_A, w_B]) \rho_K(\mathbf{r}; [w_K]) \tag{13}$$

Operators representing the densities of *chains* of species K are not an essential component of the theory, although they can be easily constructed. For example, one definition of a local chain density is obtained by averaging the monomer density contributed by type K chains of length N over the chain contour

$$\rho_{cK}(N, \mathbf{r}; [w_K]) = \frac{n_K p_K(N)}{V Q_K(N; [w_K])} \frac{1}{N} \int_0^N \mathrm{d}s\ q_K(\mathbf{r}, s)\ q_K(\mathbf{r}, N - s) = \frac{1}{N} \rho_K(N, \mathbf{r}; [w_K]) \tag{14}$$

Alternatively, one might be interested in a chain density operator defined as the density of *middle monomers* ($s = N/2$):

$$\rho_{mK}(N, \mathbf{r}; [w_K]) = \frac{n_K p_K(N)}{V Q_K(N; [w_K])} [q_K(\mathbf{r}, N/2)]^2 \tag{15}$$

All of these formulas are exact and hold beyond the mean-field approximation.

We note that a recent density functional theory of polydisperse polymers by Pagonabarraga and Cates[22] postulates that the density of monomers contributed by length N polymers and the density of *centers of mass* of length N polymer chains are related by a linear integral operation with a nonlocal kernel. In the present theory, the center-of-mass chain density does not enter, so we do not have to grapple with this nonlocality.

Finally, it is convenient to introduce the local volume fraction operators

$$\phi_K(N, \mathbf{r}; [w_K]) \equiv \rho_K(N, \mathbf{r}; [w_K])/\rho_0 = \frac{f_K p_K(N)}{\bar{N}_K Q_K(N; [w_K])} \int_0^N \mathrm{d}s\ q_K(\mathbf{r}, s)\ q_K(\mathbf{r}, N - s) \tag{16}$$

and

$$\phi_K(\mathbf{r}; [w_K]) \equiv \rho_K(\mathbf{r}; [w_K])/\rho_0 = \int_0^\infty \mathrm{d}N\ \phi_K(N, \mathbf{r}; [w_K]) \tag{17}$$

where $f_A = f$ and $f_B = 1 - f$ are the *average* volume fractions of the two species. $\phi_K(\mathbf{r})$ represents the total volume fraction of type K monomers near $\mathbf{r}$, while $\phi_K(N,\mathbf{r})$ represents the partial contribution to this volume fraction from type K chains of length N.

With the above definitions it is now possible to write explicit expressions for the first derivatives of the model Hamiltonian with respect to the chemical potential fields:

$$v_0 \frac{\delta H[w_A, w_B]}{\delta w_A(\mathbf{r})} = -f + [w_A(\mathbf{r}) - w_B(\mathbf{r})]/(2\chi) + \phi_A(\mathbf{r}; [w_A]) \tag{18}$$

$$v_0 \frac{\delta H[w_A, w_B]}{\delta w_B(\mathbf{r})} = -(1 - f) + [w_B(\mathbf{r}) - w_A(\mathbf{r})]/(2\chi) + \phi_B(\mathbf{r}; [w_B]) \tag{19}$$

These derivatives are useful in two contexts: (i) to find the equations for the saddle points of the field theory, i.e., the self-consistent mean-field theory (SCMFT) equations, and (ii) as expressions for the thermodynamic forces that are required for an "exact" numerical simulation of the model.

In the first context, the mean-field approximation is invoked by finding the "mean" fields $w_K^*(\mathbf{r})$ such that $\delta H/\delta w_K|_{w_K^*} = 0$, which implies the SCMFT equations

$$-f + [w_A^*(\mathbf{r}) - w_B^*(\mathbf{r})]/(2\chi) + \phi_A(\mathbf{r}; [w_A^*]) = 0 \tag{20}$$

$$-(1 - f) + [w_B^*(\mathbf{r}) - w_A^*(\mathbf{r})]/(2\chi) + \phi_B(\mathbf{r}; [w_B^*]) = 0 \tag{21}$$

Within this approximation, the expectation values of the

various density operators correspond to the operators themselves evaluated with $w_K \rightarrow w_K^*$, e.g.

$$\langle \phi_K(N, \mathbf{r}; [w_K]) \rangle \approx \phi_K(N, \mathbf{r}; [w_K^*]) \tag{22}$$

The saddle point fields $w_K^*(\mathbf{r})$ prove to be real quantities, so expressions such as the right-hand side of eq 22 are real as we would demand of a physical density.

Beyond the mean-field approximation, eqs 18 and 19 can be used as thermodynamic forces in a complex Langevin dynamics scheme to carry out a computer simulation of the model. Specifically, the chemical potential fields are extended to the complex plane, and fictitious Langevin dynamics is invoked to generate Markov chains of complex w_K states.[7] Simulations of this type have been reported elsewhere.[6,32] In the present paper, we restrict our analysis to the mean-field approximation.

III. Application to a Symmetric Polymer−Polymer Interface

A. Scalings for the Schulz Distribution. To illustrate the use of the present formalism, we examine a one-dimensional interface between coexisting equilibrium phases of polydisperse A and B polymers. For simplicity, we restrict our analysis to the case of a perfectly *symmetric* system in which statistical segment lengths and chain length distributions are matched, i.e. $b_A = b_B \equiv b$ and $p_A(N) = p_B(N) \equiv p(N)$. The monodisperse limit of this situation, i.e., $p(N)$ corresponding to a delta function, was considered long ago in a classic paper by Helfand and Tagami.[33] Here, we adopt a continuous Schulz chain length distribution[34]

$$p(N) = \frac{N^{\alpha-1} \exp(-N/N_a)}{N_a{}^{\alpha}\Gamma(\alpha)} \tag{23}$$

The two parameters in the Schulz distribution, α and N_a, can be related to the familiar number- and weight-average chain lengths by the following expressions:

$$N_n = \bar{N} = \alpha N_a \tag{24}$$

$$N_w = \bar{N}^2/\bar{N} = (\alpha + 1)N_a \tag{25}$$

The polydispersity index can be expressed solely in terms of the parameter α, $N_w/N_n = (\alpha + 1)/\alpha$. We emphasize that the Schulz distribution is not intrinsic to the theory but is merely a convenient and realistic chain length distribution with which to illustrate the method.

It proves convenient to rescale the contour variable s appearing in the statistical weight $q_K(\mathbf{r},s)$ by the weight-average chain length N_w. Similarly, we scale positions $\mathbf{r}$ within the system (and the simulation box size) by the unperturbed radius-of-gyration of a chain with N_w monomers: $R_{gw} = \sqrt{N_w b^2/6}$. With these scalings and by introducing rescaled chain lengths and potential fields according to $M \equiv N/N_w$ and $W_K(\mathbf{r}) \equiv N_w w_K(\mathbf{r})$, respectively, the diffusion equation in eq 7 is transformed to

$$\frac{\partial}{\partial s} q_K(\mathbf{r},s) = \nabla^2 q_K(\mathbf{r},s) - W_K(\mathbf{r})\, q_K(\mathbf{r},s) \tag{26}$$

again subject to the initial condition $q_K(\mathbf{r},0) = 1$. The partial and total species K volume fraction operators respectively become

$$\phi_K(M,\mathbf{r}; [W_K]) = \frac{(\alpha+1)^{\alpha+1} f_K M^{\alpha-1} \exp[-M(\alpha+1)]}{\alpha\Gamma(\alpha) Q_K(M; [W_K])} \int_0^M \mathrm{d}s\, q_K(\mathbf{r}, s)\, q_K(\mathbf{r}, M-s) \tag{27}$$

and

$$\phi_K(\mathbf{r}; [W_K]) = \int_0^\infty \mathrm{d}M\, \phi_K(M, \mathbf{r}; [W_K]) \tag{28}$$

The single-chain partition functions are given by $Q_K(M; [W_K]) = V^{-1} \int \mathrm{d}\mathbf{r}\, q_K(\mathbf{r},M)$.

B. Numerical Methods. In the present paper we seek one-dimensional solutions of the SCMFT eqs 20 and 21 for the saddle point fields $W_K^*(\mathbf{r})$. With the scalings introduced above, these solutions depend on only *three dimensionless parameters*: the segregation strength χN_w, the average blend composition f, and the index α in the Schulz distribution. A simple numerical way to generate the self-consistent fields is with an explicit relaxation scheme relating the jth and $(j+1)$-th approximations. The scheme involves a relaxation move toward the saddle point at the half-step[35,36]

$$W_A{}^{j+1/2}(\mathbf{r}) = W_A{}^j(\mathbf{r}) + \lambda \left[\frac{\delta H}{\delta W_B(\mathbf{r})}\right]^j$$

$$= W_A{}^j(\mathbf{r}) + \lambda\{-(1-f) + [W_B{}^j(\mathbf{r}) - W_A{}^j(\mathbf{r})]/(2\chi N_w) + \phi_B{}^j(\mathbf{r}; [W_B{}^j])\} \tag{29}$$

$$W_B{}^{j+1/2}(\mathbf{r}) = W_B{}^j(\mathbf{r}) + \lambda \left[\frac{\delta H}{\delta W_A(\mathbf{r})}\right]^j$$

$$= W_B{}^j(\mathbf{r}) + \lambda\{-f + [W_A{}^j(\mathbf{r}) - W_B{}^j(\mathbf{r})]/(2\chi N_w) + \phi_A{}^j(\mathbf{r}; [W_A{}^j])\} \tag{30}$$

followed by a constant shift of the potential fields

$$W_K{}^{j+1}(\mathbf{r}) = W_K{}^{j+1/2}(\mathbf{r}) - V^{-1} \int \mathrm{d}\mathbf{r}\, W_K{}^{j+1/2}(\mathbf{r}) \tag{31}$$

for $K = A$ and B. The second step pins the mean values of the potential fields at the origin, improving the stability of the algorithm, but has no thermodynamic consequences because the operators $\phi_K(\mathbf{r}; [W_K])$ are invariant to uniform shifts of the W_K fields. The relaxation parameter λ is adjusted to a value that reflects a compromise between rate of convergence and numerical stability. In the results reported here, fewer than 100 iterations were normally required for convergence using values of λ in the range $0.05 \le \lambda \le 1.0$.

Implementation of the above relaxational scheme requires that $\phi_K(\mathbf{r}; [W_K])$ be evaluated for the jth iterate of the field $W_K(\mathbf{r})$. According to eqs 27 and 28, this evaluation involves an indefinite integral over the normalized chain length M with an integrand that depends on the solution of the diffusion equation (26). This would seem to be a rather difficult numerical task, but it can actually be performed in an efficient manner suitable for a desktop computation. Specifically, we

employ a Gauss−Laguerre quadrature formula to evaluate the indefinite integral, i.e.

$$\int_0^\infty \mathrm{d}M \exp(-M)\, F(M) \approx \sum_{i=1}^{n_G} g_i F(M_i) \qquad (32)$$

where the abscissas (M_i) and weights (g_i) are tabulated by Abramowitz and Stegun.[37] We find that this quadrature formula converges very rapidly, so that 10 or fewer points ($n_G \lesssim 10$) are generally sufficient even for highly polydisperse systems, $\alpha < 1$.

Having settled on an n_G-point quadrature formula, the most efficient approach is to solve the diffusion equation (26) *one* time for each species K, out to a contour length coinciding with the largest Gauss−Laguerre abscissa M_{nG}. This is efficiently done with a pseudo-spectral algorithm that has its origins in quantum dynamics[38,39] and was recently applied to SCMFT calculations by Rasmussen and Kalosakas.[40] Specifically, eq 26 is integrated forward in s from the initial condition at $s = 0$ to $s = M_{nG}$ by using the formula

$$q_K(\mathbf{r}, s + \Delta s) \approx \exp[-\Delta s W_K(\mathbf{r})/2] \exp[\Delta s \nabla^2] \exp[-\Delta s W_K(\mathbf{r})/2] q_K(\mathbf{r}, s) \quad (33)$$

with errors that are third order in the contour step size Δs. The first and third propagators on the right-hand side, $\exp[-\Delta s W_K(\mathbf{r})/2]$, are applied in real space (at collocation points) where they are local, while the second propagator, $\exp[\Delta s \nabla^2]$, is applied in Fourier space by means of a fast Fourier transform (FFT). This algorithm is unconditionally stable in any number of space dimensions, is easy to code, and in our experience offers significantly higher accuracy than alternatives such as the DuFort−Frankel explicit or Crank−Nicholson semi-implicit schemes.

Having solved the diffusion equation for the longest component M_{nG} of the discretized chain length distribution function, one can then numerically evaluate the integral over s in eq 27 to obtain the partial species K volume fraction operators for $M = M_i$ with $i = 1, 2, \ldots, n_G$. These partial species volume fractions are then summed with the use of eq 32 to obtain the total species K volume fractions $\phi_K(\mathbf{r}; [W_K])$ required for the potential field updates. A Newton−Cotes formula with truncation error comparable to eq 33, i.e., Simpson's rule, is appropriate for the quadratures required in the evaluation of eq 27.

In scaling up to larger calculations in two and three dimensions, it is useful to consider the computational effort required to implement the above scheme. The number of operations required to solve the diffusion equation for the longest chain component scales as $N_s N_x \log N_x$, where N_x is the number of spatial Fourier modes (or collocation points) and $N_s = M_{n_G}/\Delta s$ is the number of contour integration steps. In turn, the number of operations required to evaluate eq 27 for all M_i is proportional to $N_s N_x \sum_{i=1}^{n_G} (M_i/M_{n_G})$, which is bounded above by $N_s N_x n_G$. Because the logarithmic factor only comes into play at very large N_x, it is evident that much of the computational burden lies in the evaluation of the density operators. Indeed, there is a dramatic advantage to using an effective quadrature scheme over the chain length distribution that converges for $n_G \lesssim 10$.

C. Results. The above numerical scheme was implemented to investigate the one-dimensional, equilibrium interface between symmetric A and B polymer phases for various values of the model parameters χN_w and α. The average volume fraction of A was fixed at $f = 0.5$ in all the results reported here. Periodic boundary conditions were imposed on a simulation box of length $L/R_{gw} = 20.0$, and calculations were performed using a spatial grid of spacing $\Delta x = 0.40$. The latter is sufficient for six-figure accuracy of the density profiles. The diffusion equation was solved using the pseudo-spectral scheme described above with a contour step Δs sufficiently small to obtain six-figure accuracy of the density profiles for the prescribed spatial resolution (in all cases $\Delta s \geq 0.0025$). At finite L, it should be noted that there is not an infinite reservoir to draw chains of different lengths from and populate the interfaces with the species weights characteristic of the thermodynamic limit. For the present illustration of the method, the fixed value of L selected was sufficiently large to obtain three-figure accuracy of the density profiles. Thus, although we report six significant figures at the prescribed L for the purpose of investigating the convergence of the Gauss−Laguerre scheme, the reader should note that these figures would change upon increasing L to approach the thermodynamic limit.

Periodic boundary conditions are particularly convenient for implementing the pseudo-spectral algorithm. However, it should be noted that such conditions mandate that the lowest energy configuration of the system contains exactly *two* A−B interfaces. All calculations reported here were performed on a desktop Pentium IV PC in the Mathematica notebook environment. In this nonoptimized environment, the typical run time to obtain a converged density profile was approximately 5 min. Evidently much better performance could be obtained by using a workstation and programming environment optimized for scientific computation.

Figure 1 illustrates how the Gauss−Laguerre scheme converges for the case of $\chi N_w = 4$ and $\alpha = 1$, which corresponds to a most probable distribution with $N_w/N_n = 2.0$. The figure shows the total species A volume fraction, $\phi_A(x)$, for varying numbers of Gauss quadrature points: $n_G = 2$, 4, 6, and 8. It is evident that the total A volume fraction profile is nearly converged with the use of only six points. This is more clearly illustrated in Table 1, which contains a tabulation of values of $\phi_A(x)$ at the midpoint of the simulation cell, $x = 0$, for various values of n_G and the Schulz distribution index α. It is interesting to note that the Gauss−Laguerre scheme actually converges slightly faster for a broader chain length distribution with $\alpha = 0.5$ ($N_w/N_n = 3$) than for narrower distributions with $\alpha = 1.0$ ($N_w/N_n = 2$) or $\alpha = 2.0$ ($N_w/N_n = 1.5$). In all cases, three-digit accuracy of $\phi_A(0)$ is obtained with the use of 10 points or fewer.

The effect of the breadth of the chain length distribution on the total A volume fraction profile is shown in Figure 2. In all cases $\chi N_w = 4$, $n_G = 10$, and $f = 0.5$. The figure shows A monomer profiles corresponding to $\alpha = 0.5$, 1.0, 2.0, and ∞ (monodisperse case). Polydispersity clearly has two principal effects: it broadens the A−B interfaces and increases the solubility of A chains in the B-rich phase and B chains in the A-rich phase. Both of these tendencies are more pronounced as the chain length distribution becomes broader, i.e., α is decreased. While these trends are well-known in quali-

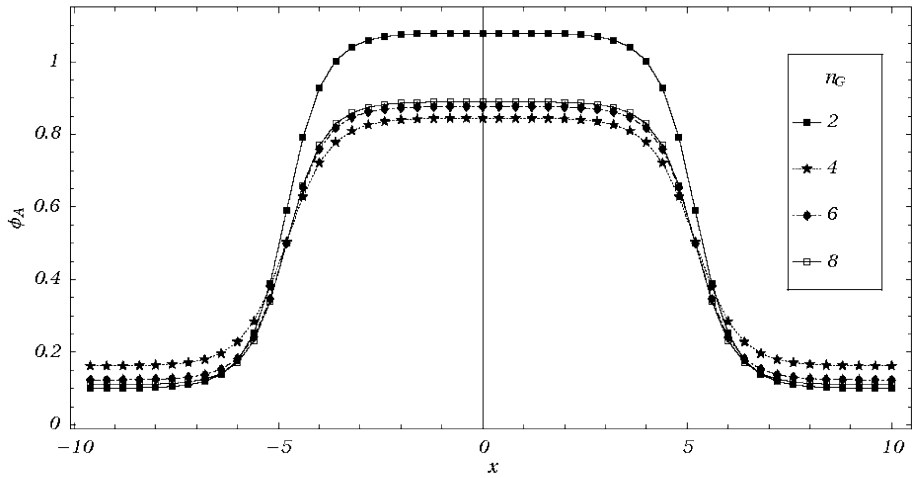

Figure 1. Convergence of total A volume fraction profile, $\phi_A(x)$, with the number of Gauss−Laguerre points. $\chi N_w = 4$ and $\alpha = 1$ in all cases. Curves correspond to $n_G = 2$, 4, 6, and 8.

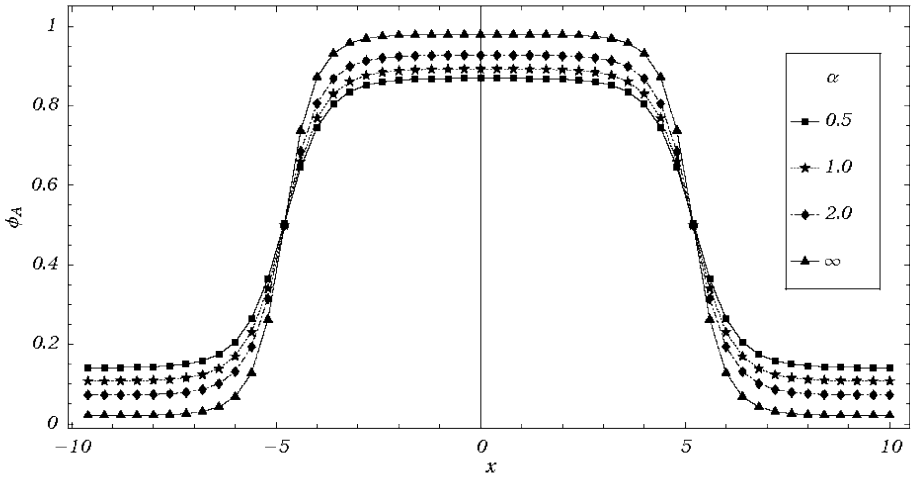

Figure 2. Influence of breadth of chain length distribution on the total A volume fraction profile. $\chi N_w = 4$ and $n_G = 10$ in all cases. Curves correspond to $\alpha = 0.5$, 1.0, 2.0, and ∞ (monodisperse case).

Table 1. Convergence of Values of $\phi_A(0)$ vs the Number of Gauss−Laguerre Quadrature Points n_G; $\chi N_w = 4.0$ and $f = 0.5$ in All Cases

	values of $\phi_A(0)$		
n_G	$\alpha = 1.0$	$\alpha = 0.5$	$\alpha = 2.0$
2	1.078 71	1.005 44	1.157 34
4	0.844 603	0.858 421	0.754 264
6	0.876 889	0.864 574	0.892 658
8	0.889 722	0.868 602	0.927 695
10	0.892 005	0.868 865	0.926 745

tative terms,[41] we are unaware of previous work that has investigated such effects in quantitative detail.

Additional insights into the structure of polydisperse interfaces can be gleaned from the *partial* volume fraction profiles. In Figure 3 we show partial A volume fraction profiles, $\phi_A(M_i,x)$, for the case of $\chi N_w = 4$ and $\alpha = 1$. The selected reduced chain lengths, M_i, coincide with the first three Gauss−Laguerre abscissas for $n_G = 8$: $M_1 = 0.170\ 27$, $M_2 = 0.903\ 70$, $M_3 = 2.251\ 08$. Also shown is the total A monomer volume fraction for the same parameters. From the shapes of the partial volume fraction profiles, we see that the shortest A chains in the distribution, i.e., those corresponding to M_1 in the figure, are only weakly localized in the A-rich phase and constitute a majority of the A species solubilized in the B-rich phase. This is as expected, since the entropy penalty associated with confinement of a species to its majority phase is largest for the smallest chains in the distribution. The longest A chains in the distribution, i.e., those corresponding to M_3 in the figure, are evidently strongly localized in the majority A phase. Another feature of Figure 3 is that the interfacial regions are disproportionately populated by the lowest molecular weight components of the distribution. This is also well-known in qualitative terms from previous work[22,41] and can be traced to the fact that there is a weak entropic attraction of chain ends to a polymer−polymer interface. Specifically, a chain end monomer at the interface need only reflect one "tail" away from the unfavorable phase, while a middle monomer must reflect two "tails" away from the disfavored phase. Because short chains have a higher concentration of end monomers than long chains, there is a net entropic attraction of the shortest chains in the distribution to the interface.

The influence of the segregation strength χN_w on the total A volume fraction profile is shown in Figure 4 for the case of a most probable distribution with $\alpha = 1$. As expected, increasing χN_w from 4 to 8 significantly narrows the A−B interfaces and increases the volume fraction of A in the A-rich phase. The latter can be understood by noting that $\chi N_w k_B T$ is the enthalpy penalty associated with exchanging an A chain of weight-average length from pure A surroundings to pure

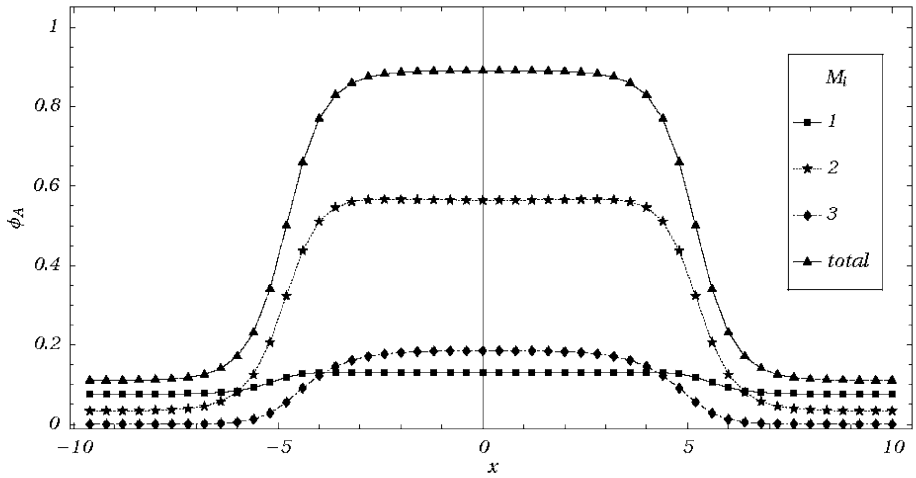

Figure 3. Partial A volume fraction profiles, $\phi_A(M_i,x)$, for the case of $\chi N_w = 4$ and $\alpha = 1$. The reduced chain lengths, M_i, coincide with the first three Gauss−Laguerre abscissas for $n_G = 8$: $M_1 = 0.170\ 27$, $M_2 = 0.903\ 70$, $M_3 = 2.251\ 08$. Also shown is the total A monomer volume fraction profile $\phi_A(x)$.

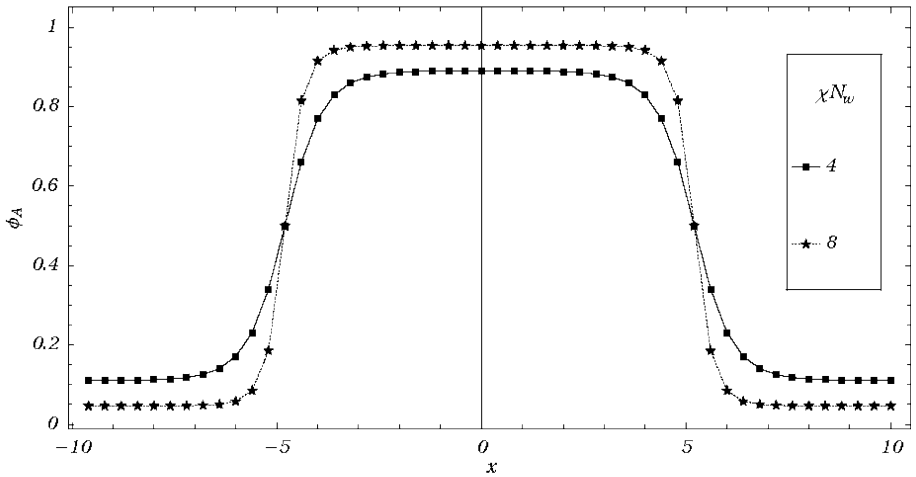

Figure 4. Influence of the segregation strength χN_w on the total A volume fraction profile. Parameters are $\alpha = 1$ and $n_G = 10$. The curves correspond to $\chi N_w = 4$ and 8.

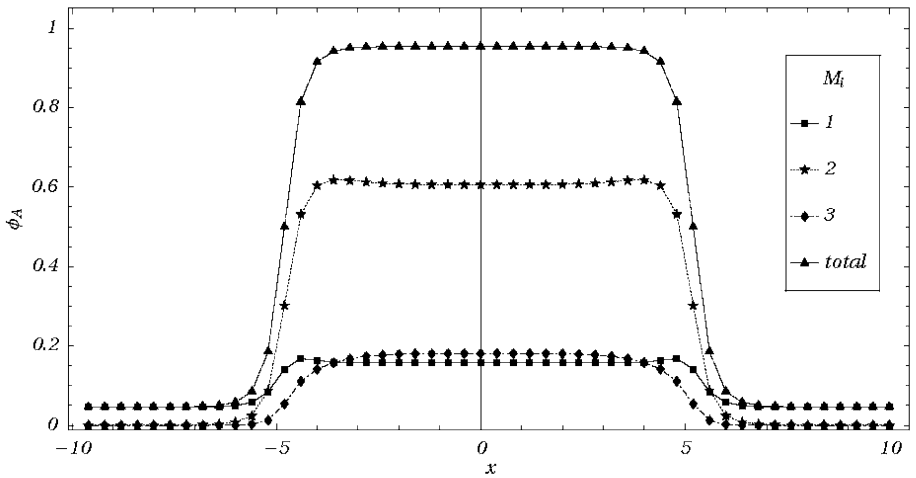

Figure 5. Partial A volume fraction profiles, $\phi_A(M_i,x)$, for the case of $\chi N_w = 8$ and $\alpha = 1$. The reduced chain lengths, M_i, coincide with the first three Gauss−Laguerre abscissas for $n_G = 8$: $M_1 = 0.170\ 27$, $M_2 = 0.903\ 70$, $M_3 = 2.251\ 08$. Also shown is the total A monomer volume fraction profile $\phi_A(x)$.

B surroundings. These trends are similar to those observed for monodisperse polymer−polymer interfaces.

Finally, in Figure 5 we show the partial A monomer density profiles for a case of stronger segregation, $\chi N_w = 8$, and with a most probable chain length distribution, $\alpha = 1$. As in Figure 3, the selected reduced chain lengths, M_i, coincide with the first three Gauss−Laguerre abscissas for $n_G = 8$: $M_1 = 0.170\ 27$, $M_2 = 0.903\ 70$, $M_3 = 2.251\ 08$. The observations of Figure 3 are still evident; i.e., the smallest A chains make up the majority of A in the B-rich phase, while the longest A chains are strongly localized in the A-rich phase.

However, more pronounced in the present case of larger χN_w is the preferential localization of short chains at the interfaces. Indeed, the curves corresponding to reduced lengths M_1 and M_2 show local maxima at each interface.

IV. Discussion and Conclusions

In the present paper, we have developed a formalism by which continuous distributions of chain length can be incorporated into field theory models of inhomogeneous polymeric fluids. These models can be solved either within the mean-field approximation (SCMFT) or by "exact" numerical simulation methods, i.e., field-theoretic computer simulations (FTS). Numerical results at the mean-field level were presented for the simple case of a symmetric interface between equilibrium coexisting phases of polydisperse A and B homopolymers. Key to the method is an efficient numerical method for evaluating the total monomer density operators for specified values of conjugate chemical potential fields. We demonstrated that a pseudo-spectral algorithm for solving the chain propagator diffusion equation can be combined with a Gauss−Laguerre quadrature formula to effectively accomplish this task. In essence, the n_G-point Gauss−Laguerre formula provides a rational way to approximate a continuous chain length distribution by a discrete distribution with n_G delta functions centered on the zeros of the n_Gth-order Laguerre polynomial. Our experience with the Schulz distribution suggests that rapid convergence can be expected so that $n_G \leq 8$ should be adequate for most situations encountered with inhomogeneous phases of polydisperse polymers.

We adopted a pseudo-spectral approach for solving the SCMFT equations in the present paper because it can be straightforwardly extended beyond the mean-field approximation, and it allows for efficient simulation of large systems whose self-assembled phases are not known in advance.[7] In some situations, however, the fully spectral approach of Matsen and Schick is preferable.[30] We expect that the spectral method for solving the mean-field equations can also be generalized with an appropriate quadrature formula to treat systems with continuous polydispersity.

While the form of the chain length distribution functions $p_K(N)$ in our theory is arbitrary, the Gauss−Laguerre formula will probably converge most rapidly for monomodal distributions such as the Schulz distribution. In cases of bi- or multimodal distributions, it is probably advantageous to first break the distribution up into two or more monomodal components, each of which is treated by a separate quadrature formula. Such extensions may prove important in treating inhomogeneous polymers produced by incomplete coupling or grafting processes and blends with discrete molecular weight fractions introduced for rheological control.

The formalism and numerical methods discussed here can be straightforwardly extended to a wide variety of inhomogeneous polymer systems. We plan to report in the near future on two- and three-dimensional calculations for polydisperse block and graft copolymers. Related models of polydisperse polymer solutions, solution blends, and graft and block copolymer solutions and alloys can be readily constructed and analyzed. It should also be straightforward to incorporate other chain models into the formalism, such as the wormlike chain or rotational isomeric state models, to treat polydisperse phases of semiflexible polymers.

Finally, we note that the present theory was intended to describe polydisperse inhomogeneous polymer phases at equilibrium. Nevertheless, the same field-theoretic models can be embedded into kinetic schemes for describing the *nonequilibrium* structure and flow behavior of inhomogeneous polymers.[42] Thus, we expect that the present formalism and numerical methods for treating polydisperse equilibrium systems will ultimately be applicable to polydisperse polymers out of equilibrium—a subject of current research interest.[43,44]

Acknowledgment. This work was partially supported by the National Science Foundation under Award DMR-98-70785 and by Atofina Chemicals. Use of the UCSB-MRSEC Central Computing Facilities supported by the NSF is also gratefully acknowledged.

References and Notes

(1) Helfand, E. *J. Chem. Phys.* **1975**, *62*, 999.
(2) Leibler, L. *Macromolecules* **1980**, *13*, 1602.
(3) Hong, K. M.; Noolandi, J. *Macromolecules* **1981**, *14*, 727.
(4) Matsen, M. W.; Schick, M. *Curr. Opin. Colloid Interface Sci.* **1996**, *1*, 329.
(5) Fraaije, J.; vanVlimmeren, B. A. C.; Maurits, N. M.; Postma, M.; Evers, O. A.; Hoffmann, C.; Altevogt, P.; GoldbeckWood, G. *J. Chem. Phys.* **1997**, *106*, 4260.
(6) Ganesan, V.; Fredrickson, G. H. *Europhys. Lett.* **2001**, *55*, 814.
(7) Fredrickson, G. H.; Ganesan, V.; Drolet, F. *Macromolecules* **2002**, *35*, 16.
(8) Holden, G., Legge, N. R., Quirk, R. P., Schroeder, H. E., Eds.; *Thermoplastic Elastomers*, 2nd ed.; Hanser/Gardner Publications: Cincinnati, OH, 1996.
(9) Jian, T.; Anastasiadis, S. H.; Semenov, A. N.; Fytas, G.; Fleischer, G.; Vilesov, A. D. *Macromolecules* **1995**, *28*, 2439.
(10) Pernot, H.; Baumert, M.; Court, F.; Leibler, L. *Nature Mater.* **2002**, *1*, 54.
(11) Chakraborty, A. K.; Shakhnovich, E. I.; Pande, V. S. *J. Chem. Phys.* **1998**, *108*, 1683.
(12) Fredrickson, G. H.; Milner, S. T.; Leibler, L. *Macromolecules* **1992**, *25*, 6341.
(13) Qi, S. Y.; Chakraborty, A. K.; Wang, H.; Lefebvre, A. A.; Balsara, N. P.; Shakhnovich, E. I.; Xenidou, M.; Hadjichristidis, N. *Phys. Rev. Lett.* **1999**, *82*, 2896.
(14) Semenov, A. N. *Eur. Phys. J. B* **1999**, *10*, 497.
(15) Sfatos, C. D.; Shakhnovich, E. I. *Phys. Rep.: Rev. Sect. Phys. Lett.* **1997**, *288*, 77.
(16) Shakhnovich, E. I.; Gutin, A. M. *J. Phys. (Paris)* **1989**, *50*, 1843.
(17) Subbotin, A. V.; Semenov, A. N. *Eur. Phys. J. A* **2002**, *7*, 49.
(18) Burger, C.; Ruland, W.; Semenov, A. N. *Macromolecules* **1990**, *23*, 3339.
(19) Erukhimovich, I.; Dobrynin, A. V. *Macromol. Symp.* **1994**, *81*, 253.
(20) Dobrynin, A. V.; Leibler, L. *Macromolecules* **1997**, *30*, 4756.
(21) Milner, S. T.; Witten, T. A.; Cates, M. E. *Macromolecules* **1989**, *22*, 853.
(22) Pagonabarraga, I.; Cates, M. E. *Europhys. Lett.* **2001**, *55*, 348.
(23) Matsen, M. W.; Bates, F. S. *Macromolecules* **1995**, *28*, 7298.
(24) Thompson, R. B.; Matsen, M. W. *Phys. Rev. Lett.* **2000**, *85*, 670.
(25) Sollich, P. *J. Phys.: Condens. Matter* **2002**, *14*, R79.
(26) Doi, M.; Edwards, S. F. *The Theory of Polymer Dynamics*; Oxford University Press: New York, 1986.
(27) deGennes, P. G. *Scaling Concepts in Polymer Physics*; Cornell University Press: Ithaca, NY, 1979.
(28) Bates, F. S.; Rosedale, J. H.; Fredrickson, G. H. *J. Chem. Phys.* **1990**, *92*, 6255.
(29) Edwards, S. F. *Proc. Phys. Soc. London* **1965**, *85*, 613.
(30) Matsen, M. W.; Schick, M. *Phys. Rev. Lett.* **1994**, *72*, 2660.
(31) Freed, K. *Adv. Chem. Phys.* **1972**, *22*, 1.
(32) Alexander-Katz, A.; Moreira, A. G.; Fredrickson, G. H. *J. Chem. Phys.*, in press.
(33) Helfand, E.; Tagami, Y. *J. Polym. Sci., Part B* **1971**, *9*, 741.
(34) Schulz, G. V. *Z. Phys. Chem. (Munich)* **1939**, *B43*, 25.
(35) Drolet, F.; Fredrickson, G. H. *Macromolecules* **2001**, *34*, 5317.

(36) Note that this off-diagonal species K relaxation is required to account for the particular orientation of the saddle point in the complex plane. In particular, H is to be minimized with respect to $W_A - W_B$ and maximized with respect to $W_A + W_B$. For more details, see ref 7.
(37) Abramowitz, M., Stegun, I. A., Eds. *Handbook of Mathematical Functions*; Dover Publications: New York, 1972.
(38) Fleck, J. A. J.; Morris, J. R.; Feit, M. D. *Appl. Phys.* **1976**, *10*, 129.
(39) Feit, M. D.; Fleck, J. A. J.; Steiger, A. *J. Comput. Phys.* **1982**, *47*, 412.
(40) Rasmussen, K. O.; Kalosakas, G. *J. Polym. Sci., Part B: Polym. Phys.* **2002**, *40*, 1777.
(41) Broseta, D.; Fredrickson, G. H.; Helfand, E.; Leibler, L. *Macromolecules* **1990**, *23*, 132.
(42) Fredrickson, G. H. *J. Chem. Phys.* **2002**, *117*, 6810.
(43) Clarke, N. *Eur. Phys. J. A* **2001**, *4*, 327.
(44) Pagonabarraga, I.; Cates, M. E. *Macromolecules* **2003**, *36*, 934.

MA034082Y